



CHORUS

This is the accepted manuscript made available via CHORUS. The article has been published as:

## Nanoparticle Superlattices as Quasi-Frank-Kasper Phases

Alex Travesset

Phys. Rev. Lett. **119**, 115701 — Published 14 September 2017

DOI: [10.1103/PhysRevLett.119.115701](https://doi.org/10.1103/PhysRevLett.119.115701)

# Nanoparticle Superlattices as Quasi-Frank-Kasper Phases

Alex Travasset\*

*Department of Physics and Astronomy, Iowa State University and Ames lab, Ames, IA, 50011*

I show that all phases reported experimentally in binary nanoparticle superlattices can be described as networks of disclinations in an ideal lattice of regular tetrahedra. A set of simple rules are provided to identify the different disclination types from the Voronoi construction, and it is shown that those disclinations completely screen the positive curvature of the ideal tetrahedral lattice. In this way, this study provides a generalization of the well-known Frank-Kasper phases to binary systems consisting of two types of particles, and with a more general type of disclinations, i.e. Quasi-Frank Kasper phases. The study comprises all strategies in nanoparticle self-assembly, whether driven by DNA or hydrocarbon ligands, and establishes the universal tendency of superlattices to develop icosahedral order, which is facilitated by the asymmetry of the particles. Besides its interest in predicting nanoparticle self-assembly, I discuss the implications for models of the glass transition, micelles of diblock polymers, and dendritic molecules, among many others.

Materials whose elementary units are nanoparticles, as opposed to atoms or molecules, provide a new form of matter organization that raises new fundamental questions and provides new opportunities to address unsolved problems. The general strategy to program the assembly of nanoparticles is to graft their surface with organic molecules, such as hydrocarbons[1], DNA[2, 3] or neutral polymers such as PEG[4] so that the combined nanoparticle-ligand system, the nanocrystal(NC), is soluble in appropriate solvents and its assembly can be controlled by external variables, such as solvent evaporation, temperature or ionic strength.

While single component NC assemble into long range structures of either fcc or bcc[2, 3, 5, 6], two component systems characterized by the parameter

$$\gamma = \frac{R_B}{R_A} \leq 1, \quad (1)$$

where  $R_A, R_B$  are the two NC radii, exhibit a fascinating cornucopia of crystalline and quasicrystalline phases[1, 7–10]: Binary nanocrystal superlattices (BNSLs).

Predicting and understanding these phases has had significant success in DNA systems[10–14]. In systems whose capping ligands are hydrocarbons, NCs often behave as hard spheres, as evidenced by the clear but rather imperfect correlation between the maximum of packing fraction (as a function of  $\gamma$ ) and the presumed equilibrium phases[1, 15, 16]. It is only recently, with the development of the Orbifold Topological Model (OTM)[17], that the circumstances under which NCs behave as hard spheres have been clarified, together with detailed quantitative predictions of the structure of each BNSL[18].

Two obvious questions then arise: are those BNSLs true minima of the free energy or just metastable states? If they are true equilibrium states, what minimal thermodynamic coordinates are needed to fully unravel the corresponding phase diagram? A possible very appealing idea is that NCs would ideally pack as regular tetrahedra, and experimental evidence exists to this statement[19], but this is possible only in curved spaces, so instead,

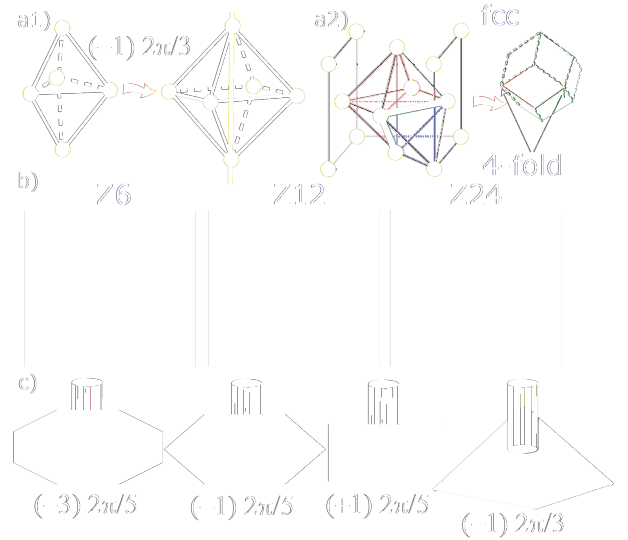


FIG. 1. a.1) Example of a  $\frac{2\pi}{3}$  disclination transforming a tetrahedra into an octahedra. a.2) The fcc lattice consists of edges (in green) sharing two tetrahedra(blue) and octahedra(red). b) Some constitutive elements (surface around a given NC) of Quasi FK phases (full list provided in SI). c) Disclinations considered in this study, see also SI.

they arrange in phases that best approximate such arrangement in flat space. The primordial example are Frank Kasper phases(FK)[20, 21], which can be regarded as decurving the ideal tetrahedral lattice (the  $\{3, 3, 5\}$  polytope) with ( $q = -\frac{2\pi}{5}$ ) disclinations[22–26]. Indeed, it has been shown that disclinations completely balance the positive curvature and satisfy the zero Regge-curvature[27] condition[24]

$$F_D = \frac{1}{2} \int R \sqrt{g} d^3x = \sum_{j=\text{edges}} \delta_j l_j = 0, \quad (2)$$

where the index  $j$  runs over all edges,  $l_j$  is the length of the disclination and  $\delta_j$  is the excess/deficit of the sum of all the dihedral angles within an edge over the flat result of  $2\pi$ .

Although the focus of this paper is on BNSLs, the consequences of this study extend to many other problems, such as general studies of the glass transition [24, 28–31], dendrimers and branched polymers[32, 33], or diblock micelles consisting of copolymers with different rigidities[34] and others[29]. Furthermore, algorithms exist to enumerate all possible lattices in terms of the disclination networks, also known as the major skeleton, that satisfy Eq. 2[35].

Assuming that the  $\{3, 3, 5\}$  polytope, which consists of 120 vertices sitting at the surface of  $S^3$ , represents the configurations in which NCs would ideally crystallize, the next question is what disclinations are available to de-curve the polytope in the flat space we live in. The rotational symmetry group of  $\{3, 3, 5\}$  is the regular icosahedral group  $\mathcal{Y}$ , which contains rotations of angles  $\frac{2\pi}{5}$  and  $\frac{2\pi}{3}$ . The former gives rise to  $\frac{2\pi}{5}q_a$  and the latter to  $\frac{2\pi}{3}q_b$  disclinations, where  $q_a, q_b$  are integers (Additional details not central to this presentation are discussed in SI). In this notation, FK phases are those whose edges (defined by nearest neighbor lattice points) consist of  $(q_a, q_b) \equiv (-1 \text{ or } 0, 0)$ . A Quasi Frank-Kasper is then defined as any crystalline or quasi-crystalline phase whose edges are characterized by general integers  $(q_a, q_b)$ .

Disclinations are more easily visualized in Voronoi representation. A  $(q_a, 0)$ -disclination threads a Voronoi face containing  $5 - q_a$  edges, see Fig. 1. The total dihedral angle is that of  $5 - q_a$  tetrahedra[24]

$$\psi_5(q_a) = (5 - q_a) \arccos(1/3). \quad (3)$$

$\frac{2\pi}{3}$  disclinations are identified from the number of edges joining a given Voronoi vertex, as shown in Fig 1. Because all vertices are joined by either 3 or 4 edges (corresponding to tetrahedra or octahedra), I interpret a  $(0, q_b)$ -disclination as the number of octahedra at a given edge. The dihedral angle is

$$\begin{aligned} \psi_3(q_b) &= -q_b (\pi - \arccos(1/3) - \arccos(1/3)) \\ &= -q_b (\pi - 2 \arccos(1/3)), \end{aligned} \quad (4)$$

where it is used that the dihedral of a regular octahedron is  $\pi - \arccos(1/3)$ . Here, the extra  $\arccos(1/3)$  arises because the angle is defined relative to the tetrahedron, and the minus sign ensures that the angle is positive. The zero curvature Eq. 2 on a BSNL unit cell is

$$\sum_{i=1}^{N_w} n_i \sum_{j=1}^{F_i} \delta_j l_j = \sum_{i=1}^{N_w} n_i \sum_{j=1}^{F_i} (2\pi - \psi_{5,j}(q_a) - \psi_{3,j}(q_b)) l_j = 0 \quad (5)$$

where  $N_w$  is the number of different Wyckoff positions of the lattice,  $n_i$  the number of NCs on each Wyckoff position,  $F_i$  the total number of faces of the  $i$ -th Voronoi cell, and  $l_j$  is the length of the corresponding disclination line. I will consider two definitions of curvature: In definition one, I assume all disclinations lengths are the same  $l_j = l_e$ . In definition 2,  $l_j$  is its value in flat space.

Lattice	$q_l$ ( $q_C = 5.1043$ )	$N_l$ ( $N_C = 13.3973$ )	$f_{ico}$
NaCl	[5.0000, 5.1716]	[12.0000, 14.4853]	0.00
CsCl	[5.1429, 5.0718]	[14.0000, 12.9282]	0.00
AuCu	[5.1429, 5.0752]	[14.0000, 12.9754]	0.00
MgZn <sub>2</sub>	[5.1000, 5.1087]	[13.3333, 13.4632]	0.90
AlB <sub>2</sub>	[5.0526, 5.1522]	[12.6666, 14.1549]	0.63
Cr <sub>3</sub> Si	[5.1111, 5.0962]	[13.5000, 13.2777]	0.89
Li <sub>3</sub> Bi	[5.1429, 5.0913]	[14.0000, 13.2051]	0.00
AuCu <sub>3</sub> *	[5.1429, 5.0114]	[14.0000, 12.1380]	0.00
Fe <sub>4</sub> C	[5.1892, 5.0321]	[14.8000, 12.3979]	0.32
CaCu <sub>5</sub>	[5.1000, 5.1110]	[13.3333, 13.4985]	0.75
CaB <sub>6</sub> *	[5.0000, 5.2196]	[12.0000, 15.3758]	0.55
bccAB <sub>6</sub> *	[5.0323, 5.3232]	[12.4000, 17.7318]	0.57
cubAB <sub>13</sub> *	[5.5000, 5.8378]	[24.0000, 95.1175]	0.44
NaZn <sub>13</sub> *	[5.1538, 5.2000]	[14.1819, 14.9935]	0.98
fcc*	[5.1043, 5.1043]	[13.3973, 13.3973]	0.00

TABLE I. Different lattices, zero curvature condition Eq. 7 using the two definitions of curvature, see discussion after Eq. 5, and degree of icosahedral order,  $f_{ico}$  Eq. 8. The asterisk\* denotes BNSLs with  $\frac{2\pi}{3}$  disclinations, where  $N_l$  does not equal the average number of nearest neighbors. Further discussion for bccAB<sub>6</sub>, cubAB<sub>13</sub> and NaZn<sub>13</sub> is provided in SI.

For example, an fcc lattice consist of Voronoi cells with four fold faces and two 4-coordinated vertices, that is  $(q_a = 1, q_b = -2)$ . There is only one Wyckoff position and Eq. 5 reads

$$\frac{F_D(\text{fcc})}{12l_{fcc}} = 2\pi - 4 \arccos(1/3) - 2(\pi - 2 \arccos(1/3)) = 0, \quad (6)$$

using either of the two definitions of the curvature. This result has the clear physical interpretation of each edge consisting of two regular tetrahedra and octahedra, see Fig. 1. Note that the same argument applies to the hcp lattice, while the bcc result is the one given by the CsCl phase. See SI for other BNSLs examples.

Using Eq. 3 and Eq. 4 into Eq. 5, the zero curvature condition becomes

$$q_l \equiv \frac{\sum_{i=1}^{N_w} n_i \sum_{j=1}^{F_i} (5 - q_a(j) + 2q_b(j)) l_j}{\sum_{i=1}^{N_w} n_i \sum_{j=1}^{F_i} (1 - q_b(j)/2) l_j} \equiv M(\gamma) = q_C, \quad (7)$$

where  $q_C = \frac{2\pi}{\arccos(1/3)} \approx 5.1042993$  is the Coxeter statistical honeycomb value[37, 38]. If all disclination lines are of the same length and of type  $(q_a, 0)$ , the quantity  $q_l$  is the average number of tetrahedra per edge, related to the average lattice coordination number by  $N_C = 12/(6 - q_C) \approx 13.3973$ [24]. In any situation, Eq. 7 and  $N_l = 12/(6 - q_l)$  can be compared against the Coxeter values, thus providing a quantitative test on the accuracy of the zero curvature condition.

In Fig. 2, the resulting disclination network is shown for the twelve most relevant BNSLs, with conventions as



FIG. 2. Twelve lattices and their respective disclination lines, drawn with the convention of Fig. 1. The radical Voronoi tessellation as implemented in Voro++[36] is used.

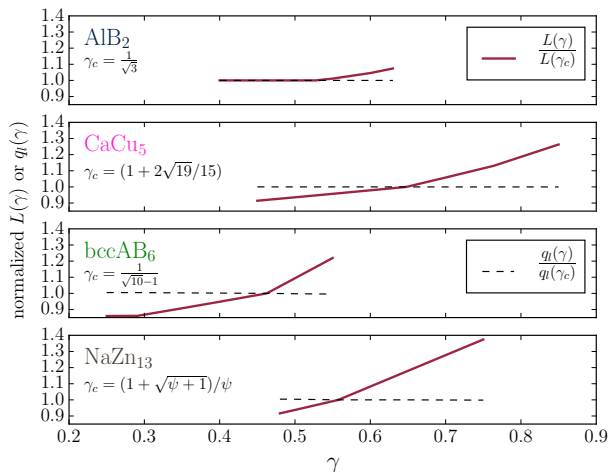


FIG. 3. Plots of  $L(\gamma)$  and  $q_l(\gamma)$ , see Eq. 7 (normalized to  $L(\gamma_c)$  and  $q_l(\gamma_c)$ , where  $\gamma_c$  is the maximum of the packing fraction, see Ref. [16]).  $L(\gamma)$  is strongly dependent on  $\gamma$ , but  $q_l$  is basically an invariant. The value of  $\psi$  ( $\text{NaZn}_{13}$ ) is provided in [18].

in Fig. 1. There are two FK phases ( $\text{MgZn}_2$  and  $\text{Cr}_3\text{Si}$ ). Particularly interesting is the  $\text{NaZn}_{13}$ , which consists of  $(0, -1$  or  $0)$ -disclinations. I label as Anti-FK any phase with that property. The accuracy of condition Eq. 7 is detailed in Table I. Rather remarkably, the two definitions of curvature, see discussion following Eq. 5, almost always bracket the statistical honeycomb  $q_C$ , and this occurs by a non-trivial cancellation of the different Voronoi cells within the BNSL unit cell (with the exception of the CsCl and AuCu). The quantity  $q_l$  is invariant, basically independent of  $\gamma$ , despite that both  $L(\gamma)$  and  $M(\gamma)$ , see Eq. 7, have a strong  $\gamma$ -dependence.

A measure of the degree of icosahedral order, defined so that  $f_{ico} = 1$  only for the  $\{3, 3, 5\}$  polytope, is

$$f_{ico} \equiv \frac{\# \text{ five-fold faces}}{\# \text{ faces}} \left( 1 - \frac{\# \text{ four-fold vertices}}{\# \text{ vertices}} \right), \quad (8)$$

defines a property of each BNSL that is independent of  $\gamma$ , with actual values are shown in Table I. Clearly, FK and anti-FK phases show the highest degree of icosahedral order, and a few phases, namely NaCl, CsCl, AuCu and AuCu<sub>3</sub> show no icosahedral order at all. Still, those phases are described by disclination networks where the two curvature values bracket the zero curvature condition, arising after a non-trivial cancellation of all the different Voronoi cells.

Contact with experiments is made in Fig. 4, where the observed phases are shown in the  $\gamma$ - $f_{ico}$  plane. The general trend is clear: for  $\gamma \lesssim 1$ , CsCl or AuCu dominate, then at around  $\gamma \approx 0.82$ , the phases with highest degree of icosahedral order begin to emerge, which gradually decreases with  $\gamma$ . The absence of icosahedral order for  $\gamma \lesssim 0.4$  and  $\gamma \gtrsim 0.8$  is a result of those regions dominated

by single component NCs (SC regime), as SC phases with icosahedral order necessarily have low packing fraction. These results illustrate that icosahedral order is facilitated by NC asymmetry for  $0.3 \lesssim \gamma \lesssim 0.82$ .

For hydrocarbon systems, the  $\text{Cr}_3\text{Si}$  phase is absent. This is expected, as for the  $\gamma$ -range where it is a FK phase the packing fraction is very low[16]. The other phases that do not conform to the general trend either consist of NCs that do not act as hard spheres, as allowed by OTM, such as AuCu<sub>3</sub>, Li<sub>3</sub>Bi and possibly Fe<sub>4</sub>C, and cubAB<sub>13</sub>, which displays unusual properties[18]. A reported A<sub>6</sub>B<sub>19</sub>[39] is not characterized with sufficient precision to be included. A quasicrystalline DDQC-AT phase is reported in Ref. [8], which combines features of AlB<sub>2</sub> and CaB<sub>6</sub>. Both phases have similar degree of icosahedral order,  $f_{ico} \sim 0.6$ , and the disclination networks contain closed loops of  $(+1, 0)$  disclinations connecting the smaller B-particles, while the larger A-A particles connect with either  $(-1, 0)$  or  $(-3, 0)$ . Another quasicrystalline phases has been recently reported[40], which competes with the  $\text{NaZn}_{13}$  phase, with high degree of icosahedral order  $f_{ico} = 0.98$  and a FK  $\sigma$ -phase.

In DNA systems[10], four phases are reported

$$\begin{array}{ccccccc} \text{CsCl} & \rightarrow & \text{AlB}_2 & \rightarrow & \text{Cr}_3\text{Si} & \rightarrow & \text{bccAB}_6 \\ \gamma & [0.75, 1.0] & [0.4, 0.6] & & [0.4, 0.5] & & [0.3, 0.4] \end{array} \quad (9)$$

which nicely follow the trend in Fig. 4. The absence of the other phases discussed arises from the need for any A(B) NC to be surrounded by as many B(A) NCs as possible to optimize DNA-hybridizations. Here, the  $\text{Cr}_3\text{Si}$  is possible because DNA stability does not require high packing fraction[11]. Recently reported assembly of bipyramid NCs Ref. [41] into FK phases suggests that disclination networks and icosahedral order is a general tendency for single component systems with different geometrical shapes, a topic that will need to be analyzed in further studies.

Recent simulations [31] have shown that the glassy state on  $S^3$  all but disappears. The clear tendency towards icosahedral order reported in this study is facilitated by the size asymmetry, thus providing another knob,  $= \gamma$ , Eq. 1 to investigate glass transitions. It also opens the possibility that the BNSLs reported to date are not true equilibrium states, but rather, those that are most easily activated. Free energy calculations with soft potentials[15, 16] and hard spheres[42] suggest that those phases are equilibrium states. Still, rigorous resolution to these questions will require additional work. Studies in  $\mu$ -sized colloidal self-assembly[43], including DNA[44, 45], where according to the OTM[18] particles cannot display non-hard sphere behaviour, may provide even better models to investigate the tendency towards icosahedral order than the NCs discussed in this study, as some phases with  $f_{ico} = 0$  become suppressed.

I thank M. Boles for a critical and very insightful

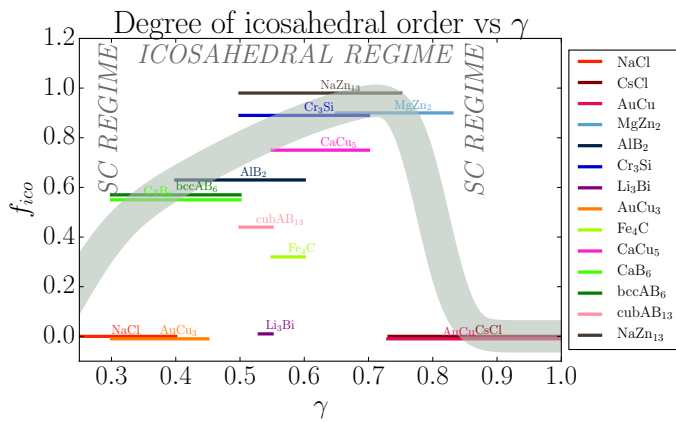


FIG. 4. Reported experimental phases over the range of  $\gamma$  for hydrocarbon[18] and DNA[10] NCs. The continuous curve is a guide to the eye illustrating the general trend. SC stands for Single Component, see discussion in text.

reading of the manuscript. This work was performed in part at Aspen Center for Physics, which is supported by NSF, PHY-1607611, and where I had many discussions with G. Grason, S. Matsumoto, R. Mosseri, J.F. Sadoc and H. Segerman. I also thank discussions and clarifications of their work with M. Boles, D. Talapin and D. Vaknin, and my students N. Horst and C. Waltmann for many insights. This work is supported by NSF, DMR-CMMT 1606336 “CDS&E: Design Principles for Ordering Nanoparticles into Super-crystals”.

\* trvsst@ameslab.gov

- [1] M. A. Boles, M. Engel, and D. V. Talapin, *Chem. Rev.* **116**, 11220 (2016).
- [2] D. Nykypanchuk, M. M. Maye, D. van der Lelie, and O. Gang, *Nature* **451**, 549 (2008).
- [3] S. Y. Park, A. K. R. Lytton-Jean, B. Lee, S. Weigand, G. C. Schatz, and C. A. Mirkin, *Nature* **451**, 553 (2008).
- [4] H. Zhang, W. Wang, S. Mallapragada, A. Travesset, and D. Vaknin, *Nanoscale* **9**, 164 (2017).
- [5] R. L. Whetten, M. N. Shafiqullin, J. T. Houry, T. G. Schaaff, I. Vezmar, M. M. Alvarez, and A. Wilkinson, *Accounts of Chemical Research*, *Acc. Chem. Res.* **32**, 397 (1999).
- [6] U. Landman and W. D. Luedtke, *Faraday Discuss.* **125**, 1 (2004).
- [7] E. V. Shevchenko, D. V. Talapin, N. A. Kotov, S. O'Brien, and C. B. Murray, *Nature* **439**, 55 (2006).
- [8] D. V. Talapin, E. V. Shevchenko, M. I. Bodnarchuk, X. Ye, J. Chen, and C. B. Murray, *Nature* **461**, 964 (2009).
- [9] M. A. Boles and D. V. Talapin, *Journal of the American Chemical Society*, *Journal of the American Chemical Society* **137**, 4494 (2015).
- [10] R. J. Macfarlane, B. Lee, M. R. Jones, N. Harris, G. C. Schatz, and C. A. Mirkin, *Science* **334**, 204 (2011), <http://www.sciencemag.org/content/334/6053/204.full.pdf>.
- [11] C. Knorowski, S. Burleigh, and A. Travesset, *Physical Review Letters* **106**, 215501 (2011).
- [12] T. I. Li, R. Sknepnek, R. J. Macfarlane, C. A. Mirkin, and M. Olvera de la Cruz, *Nano Letters* **12**, 2509 (2012), <http://pubs.acs.org/doi/pdf/10.1021/nl300679e>.
- [13] B. Srinivasan, T. Vo, Y. Zhang, O. Gang, S. Kumar, and V. Venkatasubramanian, *Proceedings of the National Academy of Sciences* **110**, 18431 (2013).
- [14] A. V. Tkachenko, *Proceedings of the National Academy of Sciences* **113**, 10269 (2016).
- [15] A. Travesset, *Proceedings of the National Academy of Sciences* **112**, 9563 (2015).
- [16] N. Horst and A. Travesset, *The Journal of Chemical Physics* **144**, 014502 (2016).
- [17] A. Travesset, *Soft Matter* **13**, 147 (2017).
- [18] A. Travesset, *ACS Nano* **11**, 5375 (2017).
- [19] B. de Nijs, S. Dussi, F. Smalenburg, J. D. Meeldijk, D. J. Groenendijk, L. Filion, A. Imhof, A. van Blaaderen, and M. Dijkstra, *Nat Mater* **14**, 56 (2015).
- [20] F. C. Frank and J. S. Kasper, *Acta Crystallographica* **11**, 184 (1958).
- [21] F. C. Frank and J. S. Kasper, *Acta Crystallographica* **12**, 483 (1959).
- [22] M. Klemm and J. F. Sadoc, *J. Physique Lett.* **40**, 569 (1979).
- [23] J. F. Sadoc and R. Mosseri, *Philosophical Magazine Part B* **45**, 467 (1982).
- [24] D. R. Nelson, *Phys. Rev. B* **28**, 5515 (1983).
- [25] D. R. Nelson and M. Widom, *Nuclear Physics B* **240**, 113 (1984).
- [26] S. Nicolis, R. Mosseri, and J. F. Sadoc, *EPL (Europhysics Letters)* **1**, 571 (1986).
- [27] T. Regge, *Il Nuovo Cimento (1955-1965)* **19**, 558 (1961).
- [28] V. Elser and C. L. Henley, *Phys. Rev. Lett.* **55**, 2883 (1985).
- [29] J. Sadoc and R. Mosseri, *Geometrical Frustration* (Cambridge University Press, 1999).
- [30] G. Tarjus, S. A. Kivelson, Z. Nussinov, and P. Viot, *Journal of Physics: Condensed Matter* **17**, R1143 (2005).
- [31] F. Turci, G. Tarjus, and C. P. Royall, *Phys. Rev. Lett.* **118**, 215501 (2017).
- [32] P. Ziherl and R. D. Kamien, *J. Phys. Chem. B* **105**, 10147 (2001).
- [33] G. M. Grason, B. A. DiDonna, and R. D. Kamien, *Physical Review Letters* **91**, 058304 (2003), copyright (C) 2007 The American Physical Society Please report any problems to prola@aps.org PRL.
- [34] S. Lee, C. Leighton, and F. S. Bates, *Proceedings of the National Academy of Sciences* **111**, 17723 (2014).
- [35] M. Dutour Sikirić, O. Delgado-Friedrichs, and M. Deza, *Acta Crystallographica Section A* **66**, 602 (2010).
- [36] C. Rycroft, *Chaos* **19**, 041111 (2009).
- [37] H. S. M. Coxeter, *Illinois Journal of Math*, 746 (1958).
- [38] H. Coxeter, *Regular Polytopes* (Dover Publications, 1973).
- [39] M. P. Boneschanscher, W. H. Evers, W. Qi, J. D. Meeldijk, M. Dijkstra, and D. Vanmaekelbergh, *Nano Letters*, *Nano Lett.* **13**, 1312 (2013).
- [40] X. Ye, J. Chen, M. Eric Irrgang, M. Engel, A. Dong, S. C. Glotzer, and C. B. Murray, *Nat Mater* **16**, 214 (2017).
- [41] H. Lin, S. Lee, L. Sun, M. Spellings, M. Engel, S. C. Glotzer, and C. A. Mirkin, *Science* **355**, 931 (2017), <http://science.sciencemag.org/content/355/6328/931.full.pdf>.
- [42] M. D. Eldridge, P. A. Madden, and D. Frenkel, *Nature*

- 365**, 35 (1993).
- [43] J. V. Sanders and M. J. Murray, *Nature* **275**, 201 (1978).
- [44] Y. Wang, I. C. Jenkins, J. T. McGinley, T. Sinno, and J. C. Crocker, *Nature Communications* **8**, 14173 (2017).
- [45] E. Ducrot, M. He, G.-R. Yi, and D. J. Pine, *Nat Mater* **16**, 652 (2017).